



Wave propagation in a wooden bar

István A. Veres *, Mahir B. Sayir

Swiss Federal Institute of Technology, Institute of Mechanical Systems, Center of Mechanics, ETH Zentrum, Zürich CH-8092, Switzerland

Abstract

In this paper we will present a method to determine the material properties of a wooden bar with rectangular cross-section using guided waves in the measurement. We modelled the wood as an orthotropic material with nine independent constants. We determined the dispersion curves theoretically in the three-dimensional case using a semi-analytical finite element method. In our laboratory we excited transversal and longitudinal waves in wooden bars of 2.5–4 m length by piezoceramic transducers. We measured the displacement or the velocity of the surface of the bar by a laser-interferometer. The dispersion curves of the bar are determined from the measurement by the linear prediction method. We related the dispersion curves and the material properties. We found the material properties by parametric model fitting.

© 2004 Published by Elsevier B.V.

Keywords: Wood; Wave propagation; Dispersion; Experiment; Fit

1. Introduction

Non-destructive testing of wood is challenging for several reasons. Wood is an anisotropic inhomogeneous material. The material properties can be evaluated by measuring the running time of the waves in the material. This method known as “time-of-flight” method uses ultrasonic waves in the high frequency range (>1 MHz) [7]. In that frequency range the waves are not dispersive, but wood has usually high damping, so the piezosignal vanishes quickly after a few centimeters range. Furthermore in this frequency range the wavelength is only few millimeters and the inhomogeneities are in the same range, thus they could disturb the measurement. By this method the material properties can be evaluated locally on a small cube [2].

In the deep frequency range (<100 kHz) the damping is lower and the wavelength is longer (few centimeters), thus the material properties can be globally evaluated on a beam and the inhomogeneities do not disturb the

measurement as much as in the high frequency range. Due to the fact that the guided waves are dispersive in this frequency range, the method of “time-of-flight” cannot be used. The dispersion curves have to be evaluated theoretically and experimentally to determine the material properties [6].

Theoretical dispersion curves for rectangular beam in the one-dimensional case can be evaluated by Euler or Timoshenko beam theory. In the three-dimensional case solutions exist only for an isotropic beam with specific aspect ratio [1]. The orthotropic three-dimensional case with rectangular cross-section was determined in [4,5] by a semi-analytical finite element method [3].

The dispersion curves can be obtained from measurement. Flexural waves will be excited by a piezoceramic transducers [6]. The waves could either be detected by a transducer [5] or by a laser-interferometer [6]. The dispersion curves can be evaluated from the measurement data by two-dimensional Fourier transformation described in [5] or by matrix pencil method like [6,12]. We will use the linear prediction method [11].

Knowing the experimental dispersion curves, the theoretical dispersion curves will be fitted. The material properties will be evaluated as model parameters of the fit [8,9].

* Corresponding author. Tel.: +41-1-632-77-56; fax: +41-1-632-11-45.

E-mail address: veres@imes.mavt.ethz.ch (I.A. Veres).

59 **2. Theoretical dispersion curves of a wooden bar**

60 *2.1. Model of the wood*

61 The structure of wood is built from natural fibers
62 oriented into the longitudinal axis of the log. The fibers
63 are arranged in annual rings. Three directions of the
64 structure with different material properties could be
65 differentiated: longitudinal, radial and tangential. Wood
66 can be modelled as a cylindrical orthotropic material
67 with nine independent material constants. Usually, a log
68 could not be measured in a laboratory, because it is too
69 large. On the other hand, wood will be commonly used
70 as a beam with rectangular cross-section. Cartesian
71 coordinates can be used for a beam, if the radii of the
72 annual rings are large compared to the dimensions of
73 the cross-section and the curvature of the rings can be
74 neglected. If the annual rings are parallel to the sides a
75 simple orthotropic model can be used, since the main
76 directions of the orthotropy are identical with the
77 directions of the sides of the bar.

78 *2.2. Semi-analytical finite element method*

79 We discretized the beam in the plane of the cross-
80 section (x - y plane) by two-dimensional finite elements.
81 The thickness of the elements is one wavelength (Fig. 1).

82 In the longitudinal direction (z) we applied harmonic
83 functions (so-called semi-analytical finite element
84 method). We used the following displacement functions:

$$\begin{aligned} u(x, y, z, t) &= N(x, y) \cos(\omega t + kz), \\ v(x, y, z, t) &= N(x, y) \cos(\omega t + kz), \\ w(x, y, z, t) &= N(x, y) \sin(\omega t + kz), \end{aligned} \quad (1)$$

86 where u , v and w are the displacements in x -, y - and z -
87 direction, $N(x, y)$ denotes the biquadratical approxima-
88 tion function, ω the angular frequency, k the wave
89 number and t the time.

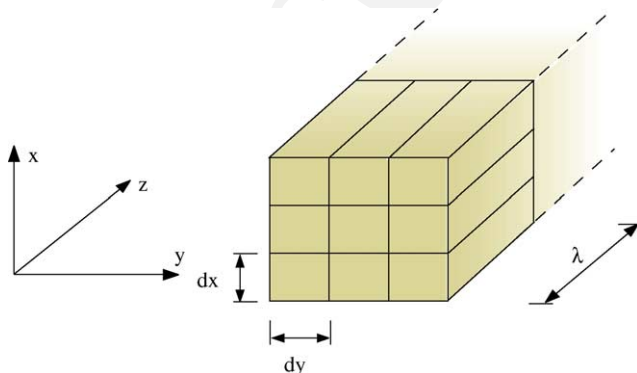


Fig. 1. Finite elements in a rectangular wooden beam.

If we formulate the finite element equations (for
example using the Rayleigh–Ritz method or like [4,5])
we get the following matrix equation:

$$\mathbf{K}\hat{\mathbf{v}} - \omega^2\mathbf{M}\hat{\mathbf{v}} = \mathbf{0}, \quad (2)$$

where the displacements of the nodes are in the vector
 $\hat{\mathbf{v}} = [\dots u_k v_k w_k \dots]^T$ ($k = 1, \dots, n$, $3n \times 3n$ is the size of the
matrices \mathbf{K} , \mathbf{M}). \mathbf{K} is the stiffness and \mathbf{M} the mass matrix.
The stiffness and mass matrices are functions of the
wave number k . Simplifying Eq. (2) leads to a general
eigenvalue problem for an arbitrary wave number k_i :

$$(\mathbf{K}(k_i) - \omega^2\mathbf{M}(k_i))\hat{\mathbf{v}} = \mathbf{0}. \quad (3)$$

The eigenvalues of this equation system are the qua-
drates of the eigenfrequencies ω_j ($j = 1, \dots, 3n$) for the
wave number k_i . Solving this eigenvalue problem for
different wave numbers k_i results in a dispersion diagram
(Fig. 2). Decomposing the stiffness matrix Eq. (2) can
also be deduced to a quadratic eigenvalue problem for
an arbitrary angular frequency ω_i :

$$(k^2\mathbf{K}_1 + k\mathbf{K}_2 + \mathbf{K}_3 - \omega_i^2\mathbf{M}')\hat{\mathbf{v}} = \mathbf{0}. \quad (4)$$

The eigenvalues are the wave numbers
 k_j ($j = 1, \dots, 6n$) for the angular frequency ω_i . The
solution (see in [10]) for different frequencies ω_i gives the
complex dispersion diagram (Fig. 3). The real part of
this diagram is identical with the dispersion diagram
resulting from Eq. (3). In our work we will apply the first
formulism of the problem.

3. Measurement of the dispersion curves

To excite waves we glued a piezo transducer to the
end of the bar. We detected the waves in the bar using
the measurement setup in [6] as shown in Fig. 4.

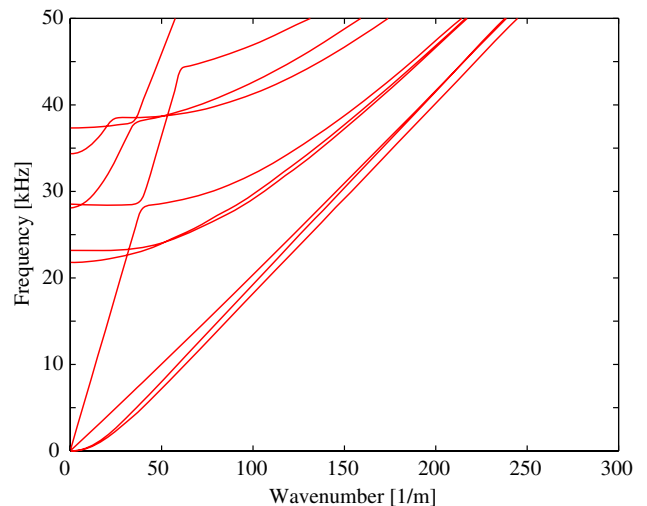


Fig. 2. Dispersion diagram of a rectangular wooden beam.

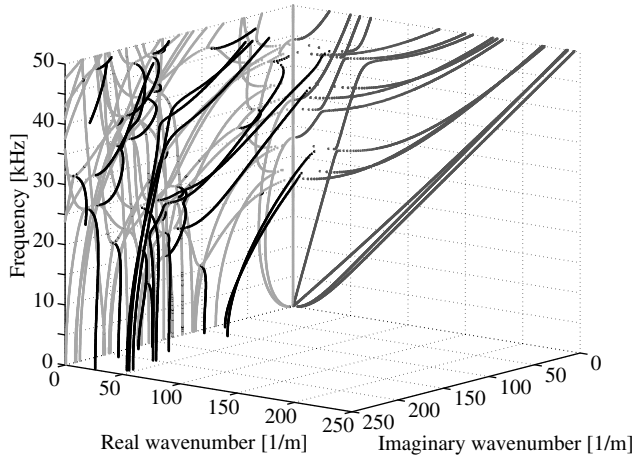


Fig. 3. Complex dispersion diagram of a rectangular wooden beam.

120 The measurement is controlled by a computer. The
 121 function generator creates a voltage signal, which is
 122 amplified and applied to the transducer. The transducer
 123 converts the voltage signal (Fig. 5a) into mechanical
 124 force at the end of the bar and excites flexural waves. We
 125 measured the displacement or the velocity at the surface
 126 of the bar by the laser-interferometer. The detected
 127 signal was filtered and recorded by the oscilloscope. The
 128 computer reads the data from the oscilloscope and
 129 stores it. The measurement is triggered by the function
 130 generator. Each measurement cycle is repeated a few
 131 hundred times and averaged to reduce the noise. A
 132 typical measurement signal and its Fourier transforma-
 133 tion can be seen in (Fig. 5b). We repeated the whole
 134 measurement process in 1500 points along the longitu-
 135 dinal axis of the bar at a distance of 0.5 mm (Fig. 6). We
 136 transformed the measurement signal into the frequency
 137 plane (using FFT). The ordinates build an exponential
 138 function for every frequency. We used the linear pre-
 139 diction method [11] to determine those functions,
 140 respectively their exponents. These exponents are related

to the wave numbers. We determined the wave numbers 141
 for a few hundred frequency points. 142

4. Estimation of material parameters 143

Between the material parameters Θ (model param- 144
 eters for the FEM model) and the measurement data \mathbf{z} 145
 (containing the frequency and the wave number) there is 146
 an implicit relationship: the dispersion relation, 147
 $\mathbf{f}(\Theta, \mathbf{z}) = \mathbf{0}$. The measurement is perturbed by an error \mathbf{e} . 148
 Thus, we substitute $\mathbf{f}(\Theta, \mathbf{z}_m + \mathbf{e}) = \mathbf{0}$, where in \mathbf{z}_m are the 149
 measured frequencies and wave numbers. 150

In our case there is no analytical relationship. 151
 Therefore a numerical calculation has to be used, for 152
 example the difference between the measured frequencies 153
 ω_m (or wave numbers \mathbf{K}_m) and the square roots of the 154
 eigenvalues in Eq. (3), ω_{eig} (or in Eq. (4), \mathbf{K}_{eig}): 155

$$\mathbf{f}(\Theta, \mathbf{z}) = \omega_m - \omega_{\text{eig}} \quad (5)$$

or 157

$$\mathbf{f}(\Theta, \mathbf{z}) = \mathbf{K}_m - \mathbf{K}_{\text{eig}}. \quad (6)$$

To fit the material parameters we used the total least 159
 squares method, where the quadrate of the error has to 160
 be minimized [8,9]: 161

$$B = (\mathbf{z}_m - \mathbf{z})^T \mathbf{Q}_{II}^{-1} (\mathbf{z}_m - \mathbf{z}), \quad (7)$$

subject to $\mathbf{f}(\Theta, \mathbf{z}) = \mathbf{0}$,

with \mathbf{Q}_{II} as a cofactor matrix. The inverted cofactor 164
 matrix can be interpreted as a weight matrix. 165

The problem can be solved by the Lagrangian mul- 166
 tipliers method. The Lagrangian function is linearized 167
 and the solution of the linearized problem is thus 168

$$\hat{\Theta} = \Theta_0 - [\mathbf{F}_\Theta^T \mathbf{F}^{-1} \mathbf{F}_\Theta]^{-1} \mathbf{F}_\Theta^T \mathbf{F}^{-1} \times [f(\mathbf{z}_0, \Theta_0) + \mathbf{F}_z(\mathbf{z}_m - \mathbf{z}_0)], \quad (8)$$

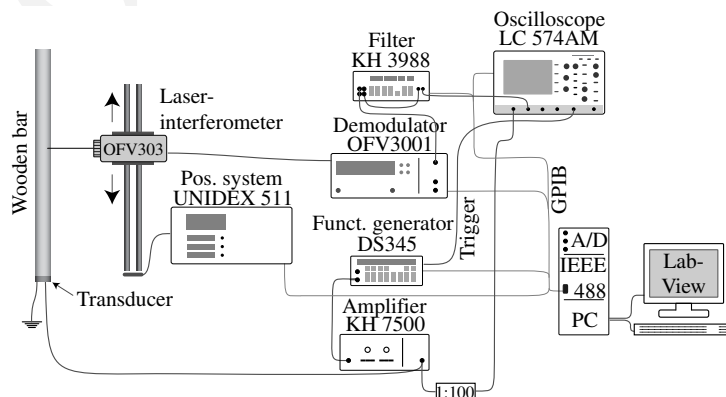


Fig. 4. Measurement setup.

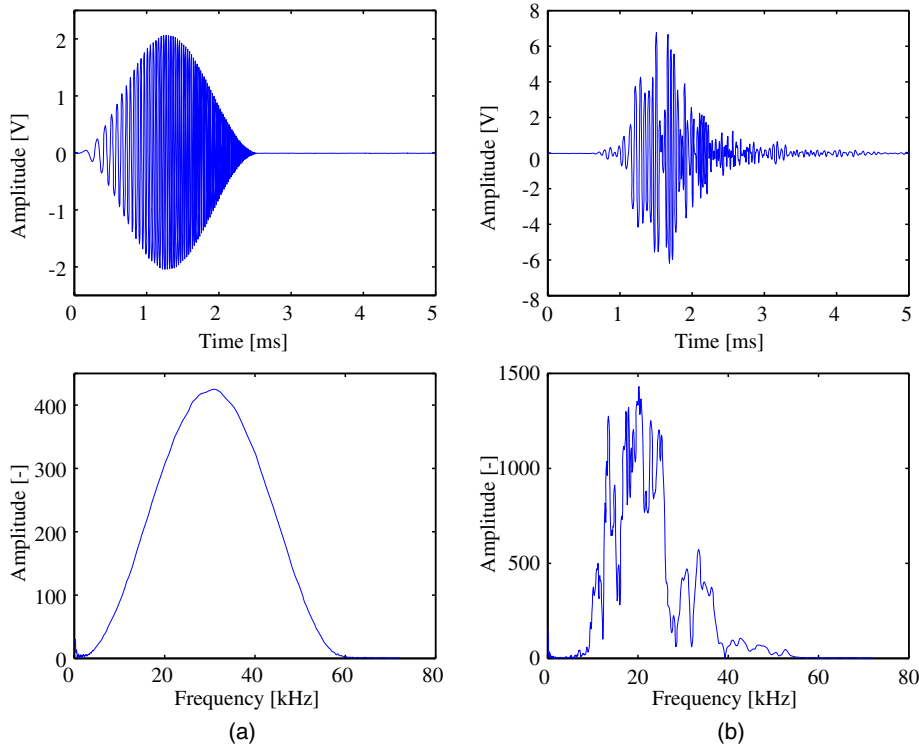


Fig. 5. (a) Exciting signal and its Fourier transformation and (b) measurement signal and its Fourier transformation.

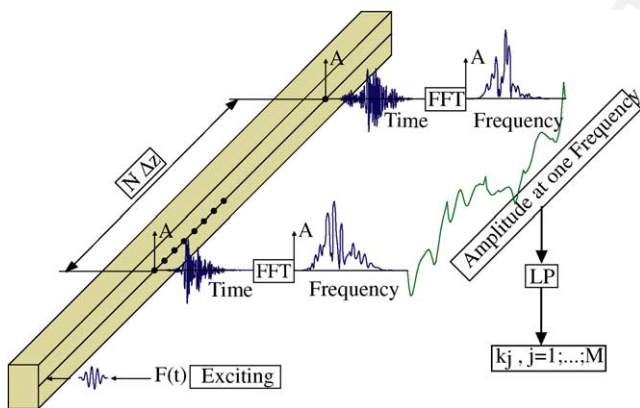


Fig. 6. Measurement and evaluation of the measurement.

$$\hat{\mathbf{z}} = \mathbf{z}_m - \mathbf{Q}_{ll} \mathbf{F}_z^T \mathbf{F}^{-1} [f(\mathbf{z}_0, \Theta_0) + \mathbf{F}_\Theta (\hat{\Theta} - \Theta_0) + \mathbf{F}_z (\mathbf{z}_m - \mathbf{z}_0)], \quad (9)$$

171 where $\mathbf{F} = \mathbf{F}_z \mathbf{Q}_{ll} \mathbf{F}_z^T$ and \mathbf{F}_Θ , \mathbf{F}_z are the Jacobians. Θ_0 and
172 \mathbf{z}_0 are the initial values. The computed values $(\hat{\Theta}, \hat{\mathbf{z}})$ are
173 only the first approximation of the solution. For the
174 iteration the values of (Θ_0, \mathbf{z}_0) have to be set equal to
175 $(\hat{\Theta}, \hat{\mathbf{z}})$ and Eqs. (8) and (9) have to be computed again.
176 The iteration process is continued until a smallness cri-
177 teria is satisfied.

178 After the initial fit the data points can be classified
179 into inlier and outlier. For the point j of the initial
180 model we used a statistical test as shown in [8]:

$$T^j = \frac{\hat{\mathbf{e}}^T \mathbf{Q}_{\hat{\mathbf{e}}\hat{\mathbf{e}}}^{-1} \hat{\mathbf{e}}^j}{p \hat{\sigma}_0^2}, \quad (10)$$

182 where $\hat{\mathbf{e}}^j$ is the actual residual vector of the point j , $\mathbf{Q}_{\hat{\mathbf{e}}\hat{\mathbf{e}}}^j$
183 the j th hyper element on the diagonal of the cofactor
184 matrix, $\hat{\sigma}_0^2$ the standard deviation and p the number of
185 dimensions of the problem. A point j is rejected on a
186 confidence level α if $T^j > F_\alpha$, with F_α being the α -quantile
187 of the Fischer distribution.

188 To collect new points we used a similar test:

$$T^k = \frac{\varpi^{kT} \mathbf{Q}_{\varpi\varpi}^{k-1} \varpi^k}{p \hat{\sigma}_0^2}, \quad (11)$$

190 where $\varpi^k = -\mathbf{f}(\hat{\Theta}, \hat{\mathbf{z}})$ and $\mathbf{Q}_{\varpi\varpi}^k$ is the k th hyper element
191 on the diagonal of the cofactor matrix [8].

5. Results

192

193 In our experiment we excited and measured flexural
194 waves in the wooden bar with a cross-section of 20×25
195 mm and density of 715 kg/m^3 . The species of the tree
196 was *Acacia Robinia*.

197 In this measurement (Fig. 7) we could identify the
198 first longitudinal mode, the first bending modes (both, in

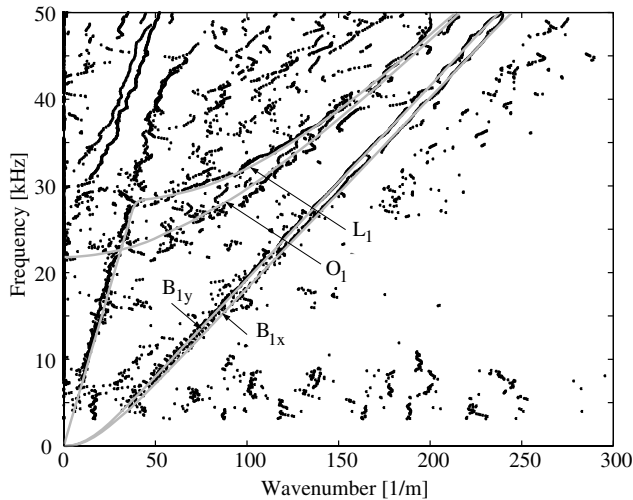


Fig. 7. Measured and calculated dispersion curves.

6. Conclusion

228

We determined the dispersion curves of an orthotropic beam with rectangular cross-section using the semi-analytical finite element method. Wood was modelled as an orthotropic material. We calculated the real and the complex dispersion curves of a wooden beam by the semi-analytical finite element method.

229
230
231
232
233
234

We also measured the dispersion curves experimentally in the deep frequency range (<100 kHz). Flexural waves were excited in a wooden bar. The waves were detected and the dispersion curves were evaluated by the linear prediction method. The agreement between the measured and the calculated dispersion curves was good (Fig. 7). We used the semi-analytical finite element model and by parametric model fitting five material constants out of the nine of a wood were determined.

235
236
237
238
239
240
241
242
243

References

244

- [1] R.D. Mindlin, E.A. Fox, Vibrations and waves in elastic bars of rectangular cross section, *Transaction of the ASME, Series E, Journal of Applied mechanics* 27 (1) (1960) 152–158.
- [2] J.L. Rose, *Ultrasonic Waves in Solid Media*, Cambridge University Press, Cambridge, 1999.
- [3] R.B. Nelson, S.B. Dong, R.D. Kalra, Vibrations and waves in laminated orthotropic circular cylinders, *Journal of Sound and Vibration* 18 (3) (1971) 429–444.
- [4] T. Mazúch, Wave dispersion modelling in anisotropic shells and rods by the finite element method, *Journal of Sound and Vibration* 198 (4) (1996) 429–438.
- [5] T. Hayashi, W.-J. Song, J.L. Rose, Guided wave dispersion curves for a bar with an arbitrary cross-section, a rod and rail example, *Ultrasonics* 41 (2003) 175–183.
- [6] D. Gsell, Nicht axialsymmetrische Wellenausbreitung in anisotropen zylindrischen Strukturen, Dissertation, ETH Zurich 2002, Diss. ETH No. 14733.
- [7] V. Bucur, *Acoustics of Wood*, CRC Publication, Boca Raton, 1995.
- [8] G. Danuser, M. Stricker, Parametric model fitting: from inlier characterization to outlier detection, *IEEE Transactions on Pattern Analysis and Machine Intelligence* 20 (2) (1998) 263–280.
- [9] H.I. Britt, R.H. Luecke, The estimation of parameters in nonlinear, implicit models, *Technometrics* 15 (2) (1973) 233–247.
- [10] F. Tisseur, K. Meerbergen, The quadratic eigenvalue problem, *Society for Industrial and Applied Mathematics* 43 (2) (2001) 235–286.
- [11] D.W. Tufts, R. Kumaresan, Estimation of frequencies of multiple sinusoids: Making linear prediction perform like maximum likelihood, *Proceedings of the IEEE* 70 (9) (1982) 975–989.
- [12] Y. Hua, T.K. Sarkar, Matrix pencil method for estimating parameters of exponentially damped/undamped sinusoids in noise, *IEEE Transactions on Acoustics Speech and Signal Processing* 38 (5) (1990) 814–824.

245
246
247
248
249
250
251
252
253
254
255
256
257
258
259
260
261
262
263
264
265
266
267
268
269
270
271
272
273
274
275
276
277
278

x - z and y - z plane), a further transversal wave mode and two higher longitudinal wave modes.

The material properties have an influence on the dispersion curves. The different wave modes are diversely influenced by the nine material parameters.

- L_1 : first longitudinal wave mode, influenced by C_{22} and C_{33} .
- B_{1x} : the first bending mode in the x - z plane, C_{33} and C_{55} influence this curve. However the influence of C_{33} is too small to fit exactly.
- B_{1y} : the first bending mode in the y - z plane, C_{33} and C_{66} influence this curve, in this case the influence of C_{33} also too small to fit exactly.
- O_1 : a transversal mode, it could not be classified as a classical bending or longitudinal wave mode. It is influenced by C_{44} .

We determined the material properties of this wood using the method described in Section 4. We calculated the dispersion diagram with these material parameters in Fig. 7 (only the four wave modes which were used to fit can be seen there). With the method described above we determined five material properties in the main diagonal of the material stiffness matrix. The three non-diagonal elements (C_{12} , C_{13} , C_{23}) of the material stiffness matrix and C_{11} have a negligible influence on the measured wave modes in this frequency range, and they could not be exactly determined.

The determined material properties are

$$\begin{aligned} C_{22} &= 1505 \text{ N/mm}^2, & C_{33} &= 15073 \text{ N/mm}^2, \\ C_{44} &= 480 \text{ N/mm}^2, & C_{55} &= 1350 \text{ N/mm}^2, \\ C_{66} &= 1410 \text{ N/mm}^2. \end{aligned}$$